Quaternary International 257 (2012) 34–42

Contents lists available at SciVerse ScienceDirect

Quaternary International

journal homepage: www.elsevier.com/locate/quaint

Geochemical and isotopic study of paleogroundwater salinization in southeastern Tunisia (Sfax basin)

Narjess Ben Cheikh [a,*], Kamel Zouari [a], Brahim Abidi [b]

[a] Laboratoire de Radio-Analyses et Environnement, Ecole Nationale d'Ingénieurs de Sfax, BP 1173, 3038 Sfax, Tunisia
[b] Arrondissement des Ressources en Eau, Commissariat Régionale au Développement Agricole de Gabès, Route de Médenine, 6019 Gabès, Tunisia

ARTICLE INFO

Article history:
Available online 25 October 2011

ABSTRACT

Salinization is a common environmental problem of groundwater contamination, particularly in developed coastal aquifers. The Sfax basin is located on the Mediterranean coast, southeastern Tunisia, and is dominated by industrial activities. The problem of groundwater mineralization in the south part of this aquifer has long been attributed to the marine influence. In this study, a combined hydrogeological and isotopic survey using chemical tracers was conducted in addition to discharge and groundwater level measurements. The results preclude seawater intrusion as an origin of groundwater mineralization. It seems that the main source of groundwater mineralization is due to the mixture with salty water lodged in the C/T (Cenomanian-Turonian) aquifer. This mixture process is carried out by the simultaneous effect of (1) a lateral flow of saline water coming from C/T aquifer in the southwest (Menzel Habib) and (2) a local vertical leakage from the same C/T formation which forms the basement of the studied aquifer. The depleted isotope signature of the majority of groundwater is characteristic of old recharge occurring during the late Pleistocene-Holocene, with the exception of some local recent refill areas.

© 2011 Elsevier Ltd and INQUA. All rights reserved.

1. Introduction

Recent hydrogeochemical research confirms that salinity constitutes the most common problem for groundwater in many coastal aquifers around the world. In relation with overexploitation, it seems that seawater intrusion remains the most widespread source of contamination of these aquifers (Leboeuf et al., 2003; Grassi et al., 2007; Jørgensen et al., 2008). Nevertheless, important contributions of other contamination phenomena such as evaporitic dissolution, vertical leakage from deeper aquifers and paleo-seawater intrusion occur (Krimissa et al., 2004; Akouvi et al., 2008; Barlow and Reichard, 2009). Threatening the groundwater resources of many Mediterranean coastal plains, this problem of seawater intrusion has been carefully studied in Tunisia, at least in the surficial aquifers (Fedrigoni et al., 2001; Trabelsi et al., 2005; Kouzana et al., 2009).

The coastal deep aquifer of Skhira (Fig. 1), located in the extreme south part of the large aquifer system of Sfax (southeast Tunisia), is characterized by the increases of the total dissolved salts (TDS) of its groundwater. It is lodged in permeable Miocene sand deposits, and is heavily exploited by the chemical industries of Skhira at the rate of 9.5 Mm^3/year (DGRE, 2006). Despite overpumping, the piezometric level of this aquifer remains above sea level. However, some studies attributed the problem of salinity to the marine influence (Maliki et al., 2000). Defined as the natural discharge zone of the aquifer of Sfax, the Skhira area constitutes an intermediate zone between three bordering aquifers known as the large aquifer of Sfax in the north, the Northern Djeffara basin in the south and the Menzel Habib aquifer in the west. The groundwater of Skhira can be considered as a mixture of waters coming from several directions. This is why concomitant sources of mineralization may be considered through a number of different pathways. Thus, it was necessary to focus on the bordering aquifers in hydraulic connection with the aquifer of Skhira so as to estimate their role in the contamination of this coastal aquifer. The complexity of this study requires the use of a multidisciplinary approach, combining hydrogeological and geochemical investigations.

2. Geological and hydrogeological setting

The study area is located in the southeastern part of Tunisia where a semiarid Mediterranean climate prevails. Its extension

* Corresponding author.
E-mail address: bencheikh_narjess@yahoo.fr (N. Ben Cheikh).

1040-6182/$ – see front matter © 2011 Elsevier Ltd and INQUA. All rights reserved.
doi:10.1016/j.quaint.2011.10.028

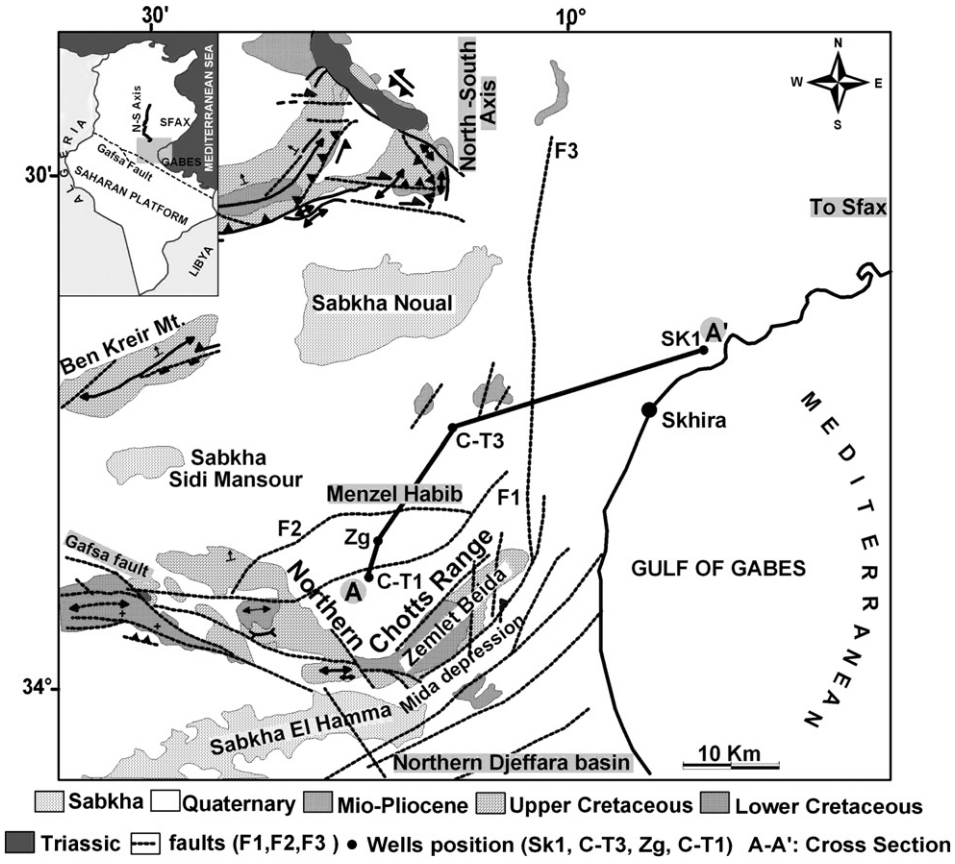

Fig. 1. Simplified geological map of the study area (Sfax, Northern Djeffara and Menzel Habib basins), showing the location of major faults and thrusts. Line A–A′ indicates the cross section shown in Fig. 2.

between Sfax, Northern Djeffara and Menzel Habib basins (Fig. 1) is marked by an obvious pluviometric regression from east (170 mm y^{-1}) to west (130 mm y^{-1}). It is bounded to the south by Sabkha El Hamma (Fig. 1), to the west by Sabkha Sidi Mansour (Fig. 1) and Ben Kreir Mountain (Fig. 1), to the north by the North–South Axis (Fig. 1) and reaches eastwards as far as the Mediterranean Sea (Fig. 1). It occupies a special position in the south of Tunisia at the boundary between the Saharan platform and the eastern part of the central Atlas of Tunisia.

It is located in the crossroads of two major tectonic features: (1) the North–South Axis (Fig. 1) which crosses the whole Atlas domain of central Tunisia extending to the Northern Chotts Range (Fig. 1) in the south. (2) The Gafsa fault (Fig. 1) represents the most salient feature of the Southern Atlas (Bouaziz et al., 2003). Geological formations present in the study area extend from the lower Cretaceous which is exposed along the Northern Chotts Range in the south to the Plio-Quaternary sediments which constitute the filling of the synclinal structures in the region (Fig. 1).

The Sfax basin is filled with Neogene and Quaternary sediments, among which, the Miocene deposits constitute an important hydrogeological sequence made up of sand and sandstone interbedded with clay. The thickness of these sand deposits decreases gradually from north (350 m in SK1 borehole) to southwest (25 m in C-T3 borehole) (Fig. 2), indicating the southern limit of the water-bearing horizons.

The basement of the Miocene deposits, in the Sfax basin, is constituted by the Upper Cretaceous (Cenomanian/Turonian). This formation, which consists of dolomites and limestones, preserves almost the same lithology toward the southwest and constitutes the principal water bearing formation in the region of Menzel Habib (Fig. 2).

In 2006, the renewable water resources of the Miocene aquifer were estimated at 23 Mm^3 with annual exploitation of about 24.7 Mm^3/year, of which 38.5% are exploited in the Skhira area (DGRE, 2006). The inter annual piezometric variation reveals a remarkable piezometric level decline varying between 0.11 m in the north and 1.48 m to the south in relation with the intensive overpumping in the Skhira area.

From geophysical explorations, the regional structural data indicate the existence of two east-west major faults (F1 and F2) (Figs. 1 and 2), which contributed to the collapse of the Menzel Habib syncline. It also highlights the existence of the transversal fault (F3) which extends longitudinally from the North–South Axis in the north to the Northern Chotts Range in the south (Fig. 1) (Amri, 2001) and plays a significant role in the lateral communication between C-T and Miocene sand deposits (Fig. 2).

The Djeffara basin covers an area of 15000 km^2 and extends from the Skhira region in the north to the Libyan border in the south. It is characterized by the variability of the water-bearing horizons. The northern part of the Djeffara basin, included in the present study, is formed by the Mio-Pliocene continental deposits made up of sands interbedded with clay. It is strongly affected by tectonic deformations which induce a distinct lateral compartmentalization (Fig. 1). The Continental Intercaliare (CI), which forms the basement of the Mio-Pliocene aquifer, is one of the largest confined aquifer

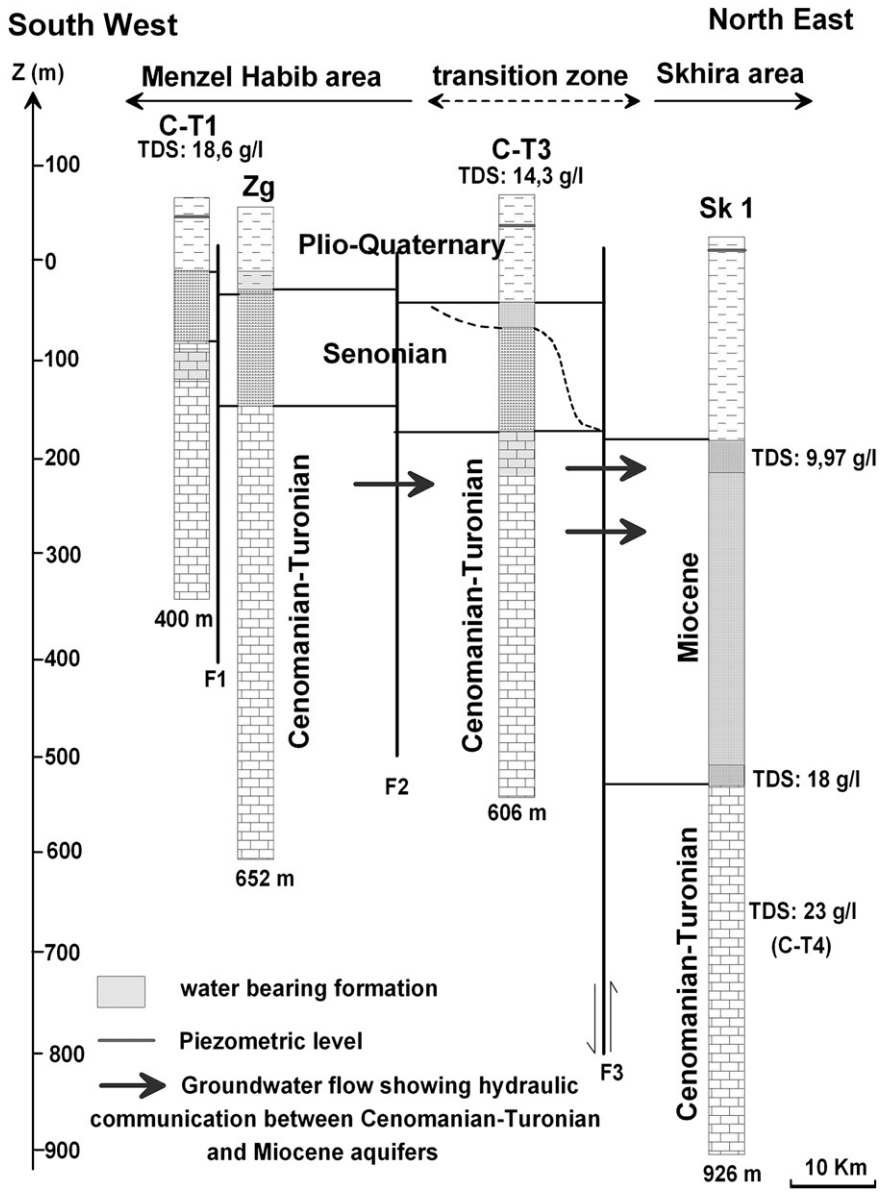

Fig. 2. Hydrogeological cross section A–A′ (for location, see Fig. 1).

systems in Tunisia. It is hosted in the continental formations of the lower Cretaceous and represents a non-renewable groundwater resource recharged during the late Pleistocene and early Holocene (ERESS, 1972; Edmunds et al., 2003).

3. Material and methods

Groundwater samples were collected from existing boreholes during a sampling campaign in January 2006 and were analyzed for ^{18}O, ^{2}H, ^{14}C and chemical analyses. The non-conservative chemical and physical parameters (temperature, pH, electrical conductivity) have been measured in the field. Major elements (Cl^-, SO_4^{2-}, Ca^{2+}, Mg^{2+}, Na^+, K^+, and HCO_3^-) were analyzed by ion liquid chromatography at the Laboratory of Radio-Analysis and Environment of the National School of Engineers of Sfax. Stable isotope compositions (^{18}O, ^{2}H) of the groundwater samples were determined by isotope ratio mass spectrometry in the Isotope Hydrology Laboratory of the International Atomic Energy Agency in Vienna and are reported in conventional notation in δ per mil with regard to the international standard V-SMOW. Radiocarbon analyses were also completed at the Laboratory of Radio-Analysis and Environment of the National School of Engineers of Sfax by using benzene synthesis and liquid scintillation spectrometry (Fontes, 1971). The measured ^{14}C concentrations are expressed as percent of modern carbon (pmc).

4. Results and discussion

4.1. Piezometric behavior

The piezometric map, established in January 2006, shows that the general groundwater flows toward the coast (Fig. 3). The piezometric levels vary in a remarkable way in relation with the structural, lithologic and especially topographic conditions.

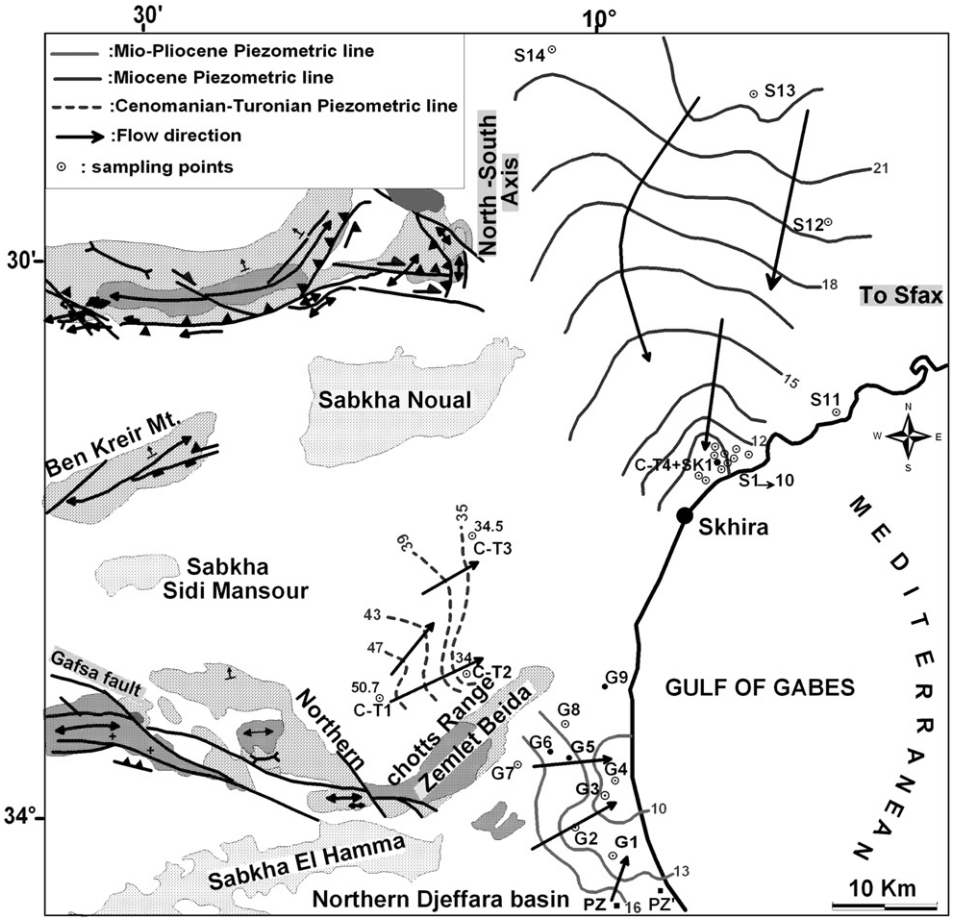

Fig. 3. Piezometric contour map (January 2006) in meters above sea level of the Miocene, Mio-Pliocene and the C-T aquifers.

In the northern part, the main groundwater flow direction is north-south. In spite of the limited number of existing boreholes, the hydraulic head of C-T aquifer reveals a southwest-northeast flow in the direction of the Skhira plain. The hydraulic communication between the C-T and Miocene aquifers, suggested by the differences of hydraulic heads, is carried out through F3 fault in accordance with the planar structure (Fig. 1). In the Northern Djeffara basin, the groundwater flow converges from the bordering mountains to the sea in several directions.

4.2. Physico-chemical data

The physical and chemical parameters indicate large spatial variation (Table 1). Water samples, collected from the Miocene aquifer, are characterized by high temperatures varying according to the borehole depth between 26 and 32.5 °C. Nevertheless, in the Northern Djeffara basin, the water temperatures vary independently from the water-bearing formation depth. They are influenced by the lateral structural compartmentalization which affects the region. In the C-T aquifer, the values of temperature are relatively more homogeneous and vary between 21 and 24.2 °C.

Groundwater samples are neutral. Their pH values are homogeneous with an average value of 7.4. The Electrical conductivity varies between 5010 and 24,200 μs/cm. These high CE measurements are correlative with the high total mineralization which varies largely between 3.9 and 23 g/l.

The salinity of the Miocene aquifer is very heterogeneous, varying between 4.4 and 13.6 g/l. It seems communally in the order of 10 g/l in the south part of the aquifer and increases with water-bearing formation depth: 13.6 g/l (between 272 and 308 m) in the S7 borehole. This vertical variation of groundwater salinity is also identified in the SK1 borehole (Fig. 2): TDS values increase from 9.97 g/l (between 200 and 237 m) to 18 g/l in the last meters of the Miocene deposits (towards 550 m) and reaches 23 g/l in the underlying middle Cretaceous limestone (C-T4). Thus, in the absence of impermeable deposits between the two horizons, this vertical stratification of groundwater salinity in the Miocene aquifer could possibly be explained by a vertical leakage from C-T aquifer considering the effect of overexploitation. The highest TDS values are measured in the Cenomanian-Turonian aquifer (C-T1, C-T2, C-T3 and C-T4).

The groundwater of Mio-Pliocene in the Northern Djeffara basin shows the lowest TDS values (average of 5 g/l). However, the increase of salinity in some points located in El Mida depression is due to the influence of highly saline waters originating from Sabkha El Hamma (Mhamdi et al., 2006).

The major ion composition of water analyses is depicted in the Piper Trilinear equivalence diagram (Fig. 4). Major elements reveal similar concentrations in C-T and Miocene aquifers, intermediate between Na^+ and Cl^- content. Thus, the C-T and Miocene groundwater belongs to the same water type: Na–Cl. In the Mio-Pliocene aquifer, the analyzed groundwater samples gets richer in Ca^{2+} and SO_4^{2-} revealing Na–Ca–Cl–SO4 water type (Fig. 4).

Table 1
Physical and chemical parameters of the analysed groundwater samples.

Well	Aquifer	Z (m)	Dep. (m)	pH	EC	T (°C)	TDS (mg/l)	Na^+ (mg/l)	Cl^- (mg/l)	SO_4^{2-} (mg/l)	K^+ (mg/l)	Ca^{2+} (mg/l)	Mg^{2+} (mg/l)	HCO^{3-} (mg/l)	CO_3^{2-} (mg/l)	IS Gyp	IS Hal	IS An	δ^2H (‰) $\delta^{18}O$(‰) V-SMOW		^{14}C (pmc)
G1	MPL	25.2	60–100	7	8320	23.2	6430	1104	2059	1944	40	624	201	195	0	−0.12	−4.37	−0.34	−59.9	−7.76	25.8 ± 1
G2	MPL	26	33–55	7.2	5010	25.1	3930	552	1136	1248	44	480	115	195	0	−0.28	−4.90	−0.50	−58.8	−7.87	
G3	MPL	13.6	65–88	7.4	5451	23.3	3960	575	1136	1363	24	384	153	189	0	−0.33	−4.88	−0.56	−53.7	−7.51	10.5 ± 2
G4	MPL	19.6	78–134	7.2	5920	21.9	4340	667	1278	1334	31	448	163	170	0	−0.30	−4.77	−0.53	−56.7	−7.69	
G5	MPL	28.6		7.2	5310	22.2	4360	519	1065	1560	16	528	163	146	0	−0.18	−4.95	−0.40	−32.3	−5.98	
G6	MPL	29.6		7.4	9130	22.5	7010	1127	2059	1800	16	784	153	164	0	−0.05	−4.36	−0.28	−37.5	−5.25	85 ± 1.7
G7	MPL	57.6		7.3	15,460	21.6	11,920	2840	3337	3816	90	480	422	213	0	−0.12	−3.79	−0.35	−35.1	−4.74	
G8	MPL	39.9	32–84	6.8	11,680	21	8820	1644	2698	2496	50	656	288	170	0	−0.06	−4.09	−0.29	−37.7	−5.41	57 ± 1
G9	MPL	11.9		7	5220	22.5	3750	455	994	1344	16	400	172	189	0	−0.32	−5.03	−0.55	−54.5	−7.36	
SK1	MS	25	200–237	7.4		29	9970	2006	3611	2826	12	650	340	99	0	−0.07	−3.90	−0.28			
S1	MS	16	196–230	7.4	12,000	26	9520	1863	2769	2544	21	384	643	207	0	−0.35	−4.05	−0.57	−39.36	−5.84	
S2	MS	20					9790	2240	3399	2527	19	703	290	85	12	−0.07	−3.88	−0.29	−41.9	−6.3	
S3	MS			7.5	12,000		9060	1851	2840	2976	35	496	451	189	0	−0.16	−4.04	−0.38	−41.35	−6.13	
S4	MS						10,800	2658	4101	2333	20	743	293	109	18	−0.10	−3.73	−0.32	−41.7	−6.3	
S5	MS	31.8	216–239	7.3	12,000		8900	1897	2698	3860	25	512	422	189	0	−0.06	−4.06	−0.28			
S6	MS	30	215–256	7.3	13,000	27.6	10,340	2012	2840	2976	28	640	432	122	0	−0.07	−4.01	−0.28	−40.81	−6.17	
S7	MS	30	272–308	7	17,000	29.3	13,640	2875	6390	1728	27	704	496	353	0	−0.32	−3.53	−0.52	−42.45	−6.16	19.5 ± 2.9
S8	MS	10	226–262	7.2	14,000	28.3	10,490	2265	3266	2736	33	480	486	189	0	−0.24	−3.90	−0.44			
S9	MS						9230	2167	3338	2225	14	643	255	128	12	−0.14	−3.90	−0.35	−41	−5.9	
S10	MS		230–260	7.3	12,000	28.4	8860	1897	2627	2784	16	416	537	237	0	−0.28	−4.07	−0.48			12.7 ± 1.7
S11	MS						9670	2194	3395	2706	15	627	291	91	6	−0.09	−3.89	−0.31			
S12	MS	48.4		8.3	5900	32.4	4450	1060	1620	927	29	230	115	102	0	−0.70	−4.48	−0.88			
S13	MS	124		8	6000	26	4750	1180	1640	845		176	260	55	0	−0.90	−4.42	−1.12			
S14	MS	103		8	14,900	32.5	9670	2181	3560	1675		333	218	36	0	−0.49	−3.88	−0.67	−45.4	−6.3	
C-T1	C-T	74	150–180	7.4	26,400	20.7	18,600	4853	7881	2760	144	1088	412	48	0	0	−3.21	−0.23	−47.80	−6.68	
C-T2	C-T	58.2	365–402	7.5	21,610	24.2	20,910	5175	8662	3000	159	1392	268	164	0	0	−3.15	−0.10	−46.50	−6.86	38 ± 1.9
C-T3	C-T	60.3	235–277	7.6	18,500	21	14,370	4088	6684	1067	53	785	130	131	0	−0.42	−3.34	−0.63			
C-T4	C-T	25		8	24,200		23,000	5520	9230	4130	150	924	905	78	0	0	−3.11	−0.22			

Z: Altitude (m), Dep.: depth of the water bearing formation (m), EC: electrical conductivity (μS/cm), TDS: total dissolved salts (mg/l), IS: saturation Indices, Gyp: gypsum, Hal: halite, An: anhydrite, MPL: Mio-Pliocene sands, MS: Miocene sands, C-T: Cenomanian-Turonian limestone.

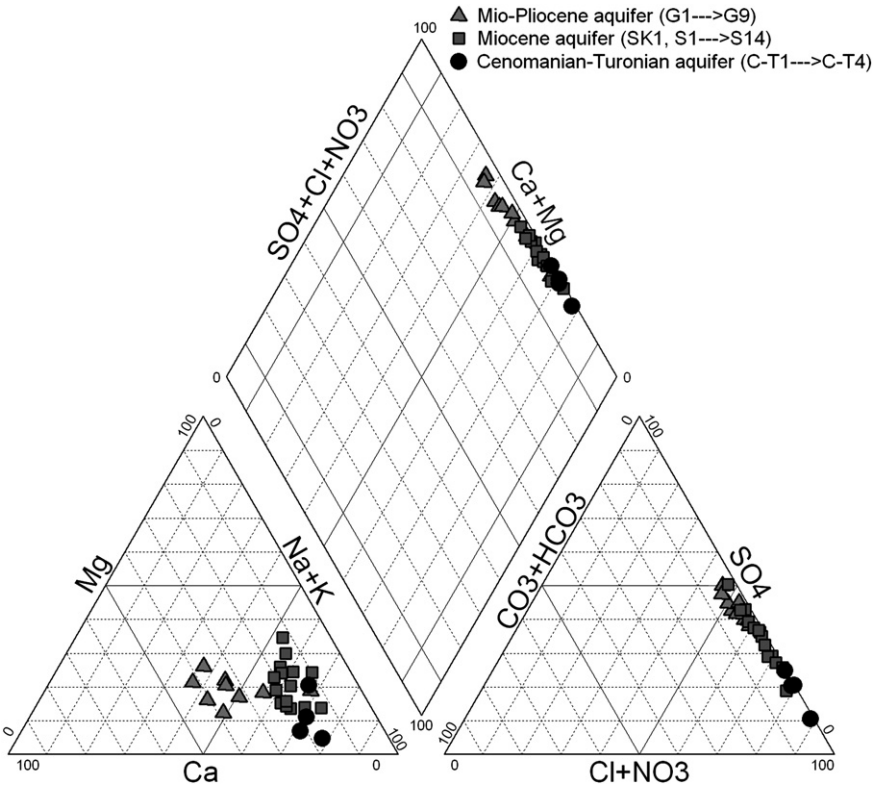

Fig. 4. Piper diagram of the analysed groundwater samples (for location of sampled points, see Fig. 3).

Bivariate diagrams of some major elements, directly related to salinity, were used in order to clarify different mechanisms that contribute to groundwater mineralization. The relationship between Na^+ and Cl^- shows that the majority of points cluster along the halite dissolution line (Fig. 5a). The dissolution of this mineral is confirmed by the negative saturation indices, indicating thus an undersaturated state (Table 1). The high values of Cl^- relative to Ca^{2+} and SO_4^{2-} contents (Fig. 5b, c), noted particularly in the C-T and Miocene aquifers, indicate the limited contribution of gypsum dissolution in the groundwater salinization. The Ca depletion relative to SO_4 content (Fig. 5d) is probably due to the cation exchange reactions which absorb Ca^{2+} on the clay fraction as Na^+ is released. Nevertheless, the C-T1, C-T2, C-T3 and C-T4 samples have a relative tendency to enrichment in Ca, which confirms the possible dissolution of carbonates in relation with their water bearing formations. On the other hand, calcium and sulphate show relative correlations with chloride in the Mio-Pliocene samples (Fig. 5c, d). Thus, it can be suggested that the increase of SO_4^{2-}, Ca^{2+} with chloride is probably due to a uniform source of gypsum/anhydrite.

4.3. Isotopic data

The stable isotope composition of water in the study area is quite variable: $\delta^{18}O$ changes from −4.7 to −7.8‰ V-SMOW with corresponding δ^2H values changing from −32.3 to −59.9‰ V-SMOW. Taken away from the pole of seawater (0‰ V-SMOW), this isotopic signature preclude seawater intrusion as an origin of groundwater mineralization. The $\delta^{18}O$ and δ^2H values (Table 1), plotted on Fig. 6 in relation with the Global Meteoric Water Line (GMWL: $\delta^2H = 8\delta^{18}O + 10$) (Craig, 1961) and the Regional Meteoric Water Line of Sfax (SMWL: $\delta^2H = 8\delta^{18}O + 13.5$) (Maliki, 2000; Jeanton et al., 2001), show that almost the totality of groundwater plots slightly near the GMWL and the SMWL.

The stable isotope signature in the Mio-Pliocene aquifer classifies the groundwater in two different groups indicating separate flow paths and recharge areas: (1) the stable isotope composition of samples located in the downstream part (G1, G2, G3, G4 and G9) of this aquifer varies from −7.8 to −7.3‰ for $\delta^{18}O$ and from −59.9 to −53.7‰ for δ^2H. These depleted isotopic signatures, consisting of low radiocarbon content (25.8 and 10.5 pmc respectively in G1 and G3), are typical of old water characteristic of the CI (Continental Intercalaire) aquifer (average stable isotope compositions are respectively −8.16‰ for $\delta^{18}O$ and −61.2‰ for δ^2H (ERESS, 1972; Abidi, 2001; Edmunds et al., 2003)). (2) In the upstream part (G5, G6, G7 and G8), the measured stable isotope composition ranges from −5.9 to −4.7‰ for $\delta^{18}O$ and from −37.7 to −32.3‰ for δ^2H, suggesting recent recharge water originating from Zemlet El Beida mountains in agreement with flow direction. This is also confirmed by the high ^{14}C contents (57 and 85 pmc respectively in G8 and G6 boreholes). The two samples representing the Cenomanian-Turonian aquifer (C-T1 and C-T2) are characterized by average values of −47‰ and −6.7‰, for δ^2H and $\delta^{18}O$, respectively. In the Skhira basin, stable isotope contents are quite homogenous. The $\delta^{18}O$ and δ^2H values range respectively from −6.3 to −5.8‰ and from −45.4 to −39.6‰. The similarity between the isotopic composition of the Miocene groundwater and those meeting in the C-T aquifer supports the hypothesis of the mixing process between the Cenomanian-Turonian aquifer in the west and the Miocene aquifer of Sfax (average stable isotope compositions are respectively −6.1‰ for $\delta^{18}O$ and −40.8‰ for δ^2H (Maliki, 2000)) in agreement with piezometric data. This mixing process seems to be controlled by

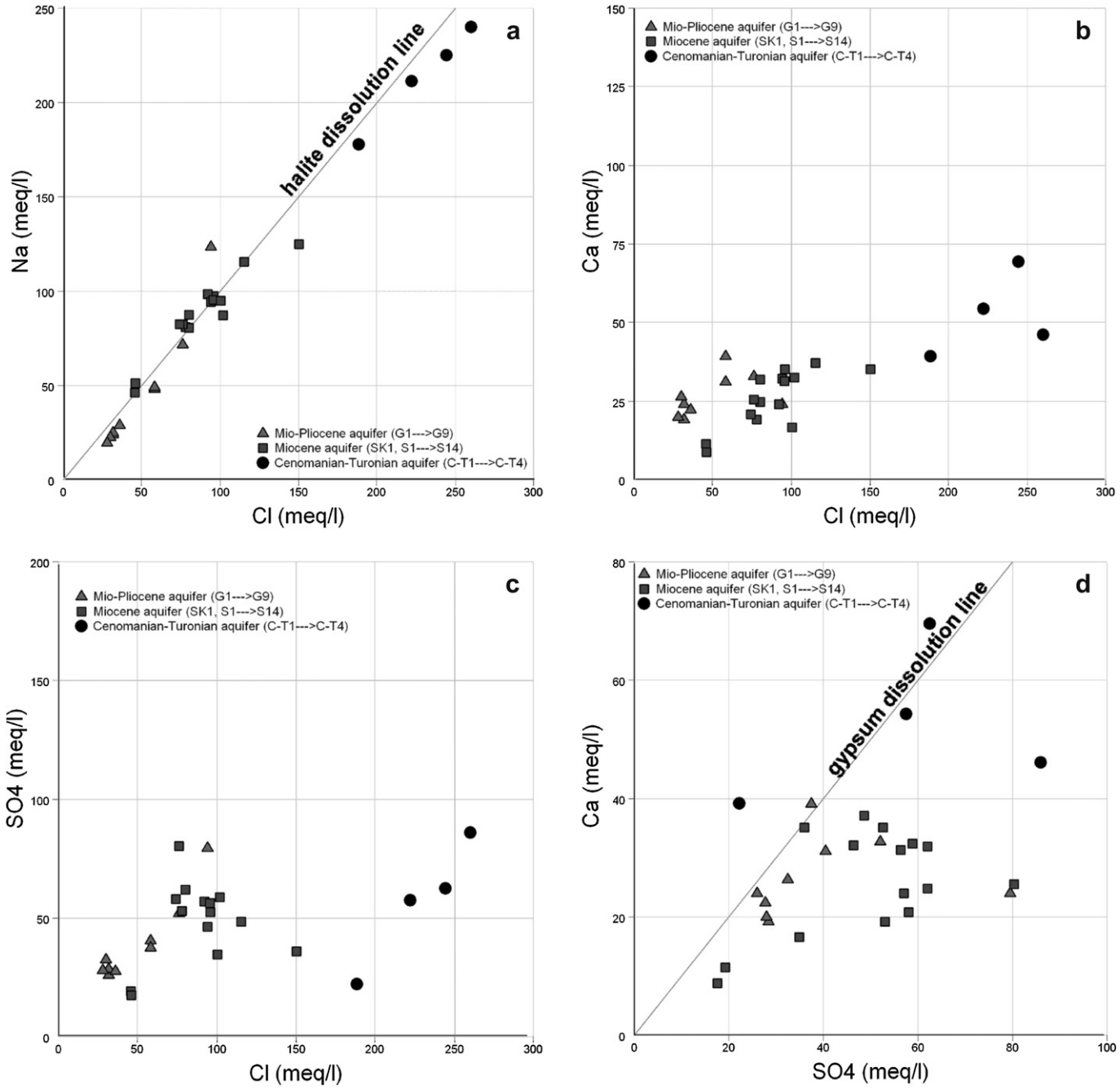

Fig. 5. Relationships between major elements in the analysed groundwater samples: Na/Cl (a), Ca/Cl (b) SO_4/Cl (c) and Ca/SO_4 (d) (for location of sampled points, see Fig. 3).

tectonic features. Accordingly, the isotopic composition of samples collected from the Mio-Pliocene aquifer (Northern Djeffara basin) shows the autonomy of this aquifer in absence of any significant hydrodynamic continuation with bordering aquifers (C-T and Miocene aquifers).

More information is obtained by plotting chloride content versus $\delta^{18}O$ (Fig. 7). The water samples collected from the Mio-Pliocene aquifer are divided into two poles with the same distribution observed in Fig. 7: (1) the pole corresponding to the old water, resulting from mixture with Continental Intercalaire groundwater, has average values of 37.2 meq/l and 7.63‰ versus V-SMOW, respectively in chloride and $\delta^{18}O$. (2) The second pole, characteristic of a recent recharge, shows that the increase of Cl contents is accompanied with the $\delta^{18}O$ enrichment. This is due to the effect of rainwater infiltration materialized through Zemlet El Beida Mountain and to the contribution of saline water originating from Sabkha El Hamma. On the other hand, the increase of Cl contents in the Miocene groundwater is further evidence that supports their mixture with C-T groundwater.

The depleted isotope signature of the majority of samples in the study area shows that the groundwater was recharged under

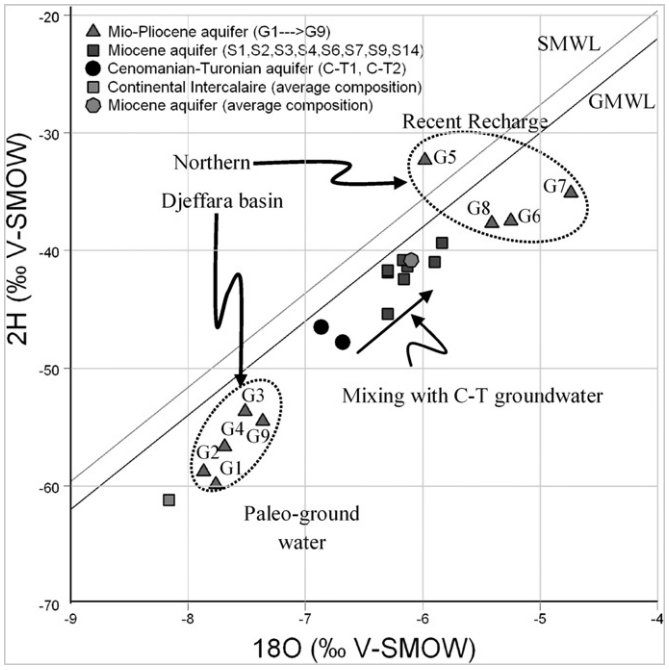

Fig. 6. The δ^2H–$\delta^{18}O$ relationship of Cenomanian-Turonian, Miocene and Miopliocene groundwaters (for location of sampled points, see Fig. 3).

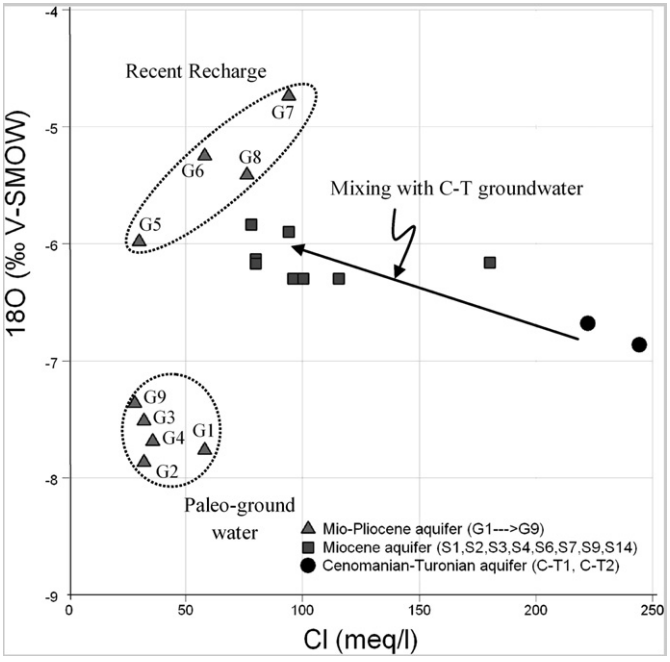

Fig. 7. $\delta^{18}O$/Cl relationship of C-T, Miocene and Mio-Pliocene groundwaters (for location of sampled points, see Fig. 3).

distinctly different climatic conditions, during late Pleistocene and early Holocene (Fig. 8). This is consistent with negligible radiocarbon content. However, the upstream part of the Mio-Pliocene aquifer seems to be characterized by a local recent recharge (G6 and G8) from the bordering mountains.

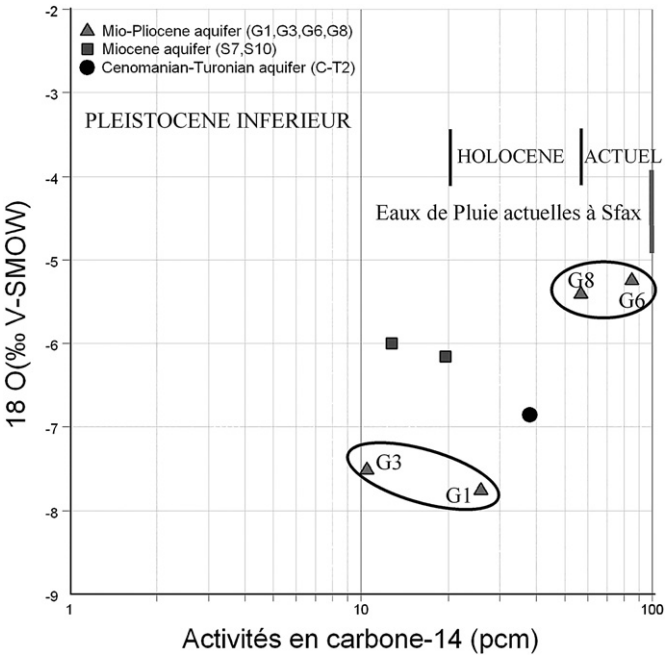

Fig. 8. $\delta^{18}O/^{14}C$ relationship of C-T, Miocene and Mio-Pliocene groundwaters.

5. Conclusion

The coastal deep aquifer of Skhira belongs to the large aquifer system of Sfax, and is lodged in the Miocene sand deposits. In spite of the high salinity of its groundwater, this coastal aquifer represents an important socio-economic interest in the region.

This study presents the results of several isotopic and chemical tools in an attempt to reveal the origin of groundwater mineralization in the coastal deep aquifer of Skhira. The results allow the exclusion of the hypothesis of seawater intrusion as an origin of groundwater mineralization. Piezometric data combined with the geochemical analyses of groundwaters confirm the hydraulic connection between the Cenomanian-Turonian aquifer and Miocene aquifer. It seems that the high groundwater salinity of the coastal aquifer of Skhira can be attributed to the simultaneous effect of: (1) a lateral contamination from saline water of the Cenomanian-Turonian aquifer in the southwest (Menzel Habib) and (2) local vertical leakage from the same aquifer (C-T) which forms the basement of the Miocene deposits. Nevertheless, the Miocene aquifer in the south, threatened locally by the contribution of saline waters from Sabkha El Hamma, appears to be hydrodynamically isolated from the bordering aquifers (Menzel Habib and Sfax). On the other hand, isotopic data clearly reveal the depleted signature of the majority of the groundwater, in the exception of samples collected in the upstream part of the Northern Djeffara basin which reflect recent infiltrated water.

Acknowledgements

The authors gratefully acknowledge the contributions of the staff members of Gabes and Sfax Water Resources Division/Agriculture Ministry, for their help during field Work. We thank technical staff at the Laboratory of the International Agency of Atomic Energy (IAEA) and the Laboratory of Radio-Analyses and Environment of the National Engineering School of Sfax (ENIS) for their help during laboratory analyses.

References

Abidi, B., 2001. La nappe du Continental Intercalaire du Sud-Est Tunisien: Analyses de la situation actuelle. DGRE, 111 p.

Akouvi, A., Dray, M., Violette, S., Marsily, G., Zuppi, G.M., 2008. The sedimentary coastal basin of Togo: example of a multilayered aquifer still influenced by a palaeo-seawater intrusion. Hydrogeology Journal 16, 419–436.

Amri, F., 2001. Note géophysique sur les possibilités d'implantation d'un forage profond dans la région de Menzel Habib (Gabès). 25 p.

Barlow, P.M., Reichard, G., 2009. Saltwater intrusion in coastal regions of North America. Hydrogeology Journal. doi:10.1007/s10040-009-0514-3.

Bouaziz, S., Jedoui, Y., Barrier, E., Angelier, J., 2003. Neotectonic in the Tyrrhenian marine deposits of the southeastern Tunisian coast: implications for sea level changes. Comptes Rendues Geoscience, 247–254.

Craig, H., 1961. Isotopic variations in meteoric water. Science 133, 1702–1703.

Direction Générale des Ressources en Eau (DGRE), annuaire d'exploitation des nappes profondes, 2006.

ERESS, 1972. Etude des ressources en eau du Sahara Septentrional. UNESCO, Paris.

Edmunds, W., Guendouz, A., Mamou, A., Moulla, A., Shand, P., Zouari, K., 2003. Groundwater evolution in the Continental Intercalaire aquifer of southern Algeria and Tunisia: trace and isotopic indicators. Applied Geochemistry 18, 805–822.

Fedrigoni, L., Krimissa, M., Zouari, K., Maliki, A., Zuppi, G., 2001. Origine de la minéralisation et comportement hydrogéochimique d'une nappe phréatique soumise à des contraintes naturelles et anthropiques sévères: exemple de la nappe Djebeniana (Tunisie). Géosciences de surface, 665–671.

Fontes, J.C., 1971. Un ensemble destiné à la mesure de l'activité du radiocarbone naturel par scintillation liquide. Revue Geographie Physique et Geologie Dynamique 13, 67–86.

Grassi, S., Cortecci, G., Squarci, P., 2007. Groundwater resource degradation in coastal plains: the example of the Cecina area (Tuscany-Central Italy). Applied Geochemistry 22, 2273–2289.

Jeanton, H., Zouari, K., Travi, Y., Daoud, A., 2001. Caractérisation isotopique des pluies en Tunisie. Essai de typologie dans la région de Sfax. Earth and Planetary Science Letters 333, 625–631.

Jørgensen, N., Andersen, M., Engesgaard, P., 2008. Investigation of a dynamic seawater intrusion event using strontium isotopes ($^{87}Sr/^{86}Sr$). Journal of Hydrology 348, 257–269.

Kouzana, L., Ben Mammou, A., Felfoul, M., 2009. Seawater intrusion and associated processes: case of the Korba aquifer (Cap-Bon, Tunisia). Comptes Rendues Geoscience 341, 21–35.

Krimissa, S., Michelot, J., Bouchaou, L., Mudry, J., Hsissou, Y., 2004. Sur l'origine par altération du substratum schisteux de la minéralisation chlorurée des eaux d'une nappe côtière sous climat semi-aride (Chtouka-Massa, Maroc). Comptes Rendues Geoscience 336, 1363–1369.

Leboeuf, P., Bosch, A., Calvache, M., Vallejos, A., Andreu, J., 2003. Strontium, SO_4^{2-}/Cl^- and Mg^{2+}/Ca^{2+} ratios as tracers for the evolution of seawater into coastal aquifers: the example of Castell de Ferro aquifer (SE Spain). Comptes Rendues Geoscience 335, 1039–1048.

Maliki, A., 2000. Etude hydrogéologique, hydrochimique et isotopique de la nappe profonde de Sfax. PhD thesis, University of Tunis. 254p.

Maliki, A., Krimissa, M., Michelot, J., Zouari, K., 2000. Relation entre nappes superficielles et aquifère profond dans le bassin de Sfax (Tunisie). Comptes Rendues. Géosciences de surface 331, 1–6.

Mhamdi, A., Gouasmia, M., Gasmi, M., Bouri, S., Ben Dhia, H., 2006. Évaluation de la qualité de l'eau par application de la méthode géoélectrique: exemple de la plaine d'El Mida–Gabes Nord (Sud tunisien). Comptes Rendues. Géosciences de surface 338, 1228–1239.

Trabelsi, R., Zairi, M., Smida, H., Ben Dhia, H., 2005. Salinisation des nappes côtières: cas de la nappe nord du Sahel de Sfax, Tunisie. Comptes Rendues Geoscience 337, 515–524.